

1,3-Di-peptido-conjugates of calix[4]arene and its di-OCH₃ derivatives: Synthesis, characterization and phosphate recognition

Mishtu Dey, Amjad Ali, Amitabha Acharya & Chebrolu P Rao*

Bioinorganic Laboratory, Department of Chemistry, Indian Institute of Technology Bombay, Powai, Mumbai 400 076, India

E-mail: cp rao@iitb.ac.in

Received 21 October 2009; accepted (revised) 3 June 2010

Novel double-armed peptido-conjugates of calix[4]arene have been developed on the lower rim of the macrocycle. The functional group pendants exhibit conformational bend through the involvement of 11-atom N-H...O hydrogen bond inscribed in a 14-atom O-H...O interaction. As a result, only the terminal -COOR and -COOH groups are exposed to the environment, but not the amide moiety. The *cone*-conformation of the calix[4]arene is further stabilized through the O-H...O interactions at the lower rim. In effect, the conjugates exhibit a binding core at the lower rim along with hydrophobic cavity formed by the enclosure of arene moieties. Conformational mobility induced by the replacement of lower rim phenolic-OH by -OCH₃ has also been demonstrated by variable temperature NMR studies in case of the corresponding -OCH₃ derivatives. Differential receptor binding characteristics of these conjugates towards phosphate are demonstrated using absorption spectroscopy. The negatively charged phosphate group is received preferentially by the carboxylic terminal over the ester terminal conjugate.

Keywords: Peptido-conjugates of calix[4]arene, HMQC, binding core, conformational mobility, phosphate binding

Calix[4]arene possesses ubiquitous properties of having both hydrophilic and hydrophobic compartments^{1,2} together in the same molecule besides possessing an arene cavity^{3,4}, at least in *cone*-conformation, capable of trapping a variety of small species and hence are important in building model systems for biomimetic studies^{5,6}. Further, these molecules can be easily modified by derivatizing either at the hydrophilic lower rim or at the hydrophobic upper rim⁷ to result in the compounds of interest as receptors towards neutral as well as ionic species^{8,9}. Thus the resultant calix[4]arene-conjugates exhibit not only the characteristics of the individual partners present in it, but also several newer ones that requires the presence of both the units together. It is these properties that may provide novel characteristics to the resultant conjugates and thereby entice chemists to exploit such properties in order to answer several queries in the pertinent field. In this context it is intended to modify 1,3-positions of calix[4]arene to result in the conjugates of amino acids *via* amide linkage in order to explore their potential as receptors towards organic and inorganic guests and thereby act as bioorganic and bioinorganic models. In this regard, the present paper demonstrates the development of 1,3-disubstituted conjugates of Gly, Ala, Glu and Asp

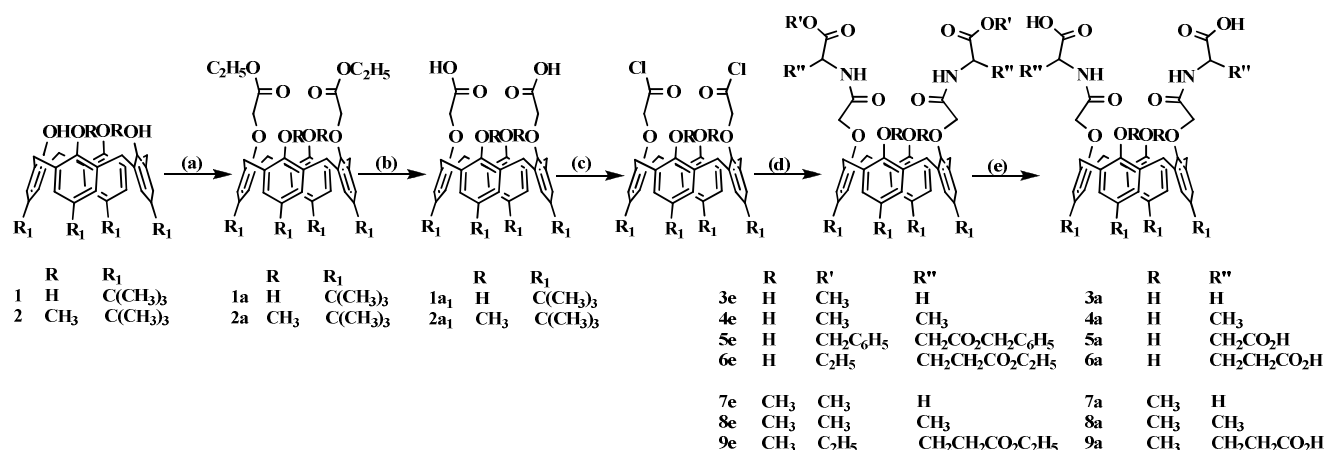
residues with calix[4]arene, and Gly, Ala and Glu residues with 1,3-di-OMe-calix[4]arene¹⁰⁻¹². The products have been characterized thoroughly, and the structure of the Gly-conjugate was established by single crystal X-ray diffraction. Further the conjugates was explored for their receptor properties towards organic phosphates.

Results and Discussion

A series of lower rim 1,3-di-amino acid conjugates of calix[4]arene have been synthesized either starting from *p*-*tert*-butyl-calix[4]arene or its di-OMe derivative in four or five steps respectively, to result in the products having terminal carboxylic ester (**3e-6e** and **7e-9e**) or carboxylic acid (**3a-6a** and **7a-9a**) as shown in **Scheme I**. All the compounds were characterized satisfactorily by FTIR, ¹H and ¹³C NMR, ¹H-¹H COSY, ¹H-¹³C HMQC and mass spectra (Experimental Section).

Characterization

Comparison of the melting points (m.p.) of the conjugates showed an increase in the m.p. for the -COOH conjugates **3a-6a** as compared to the corresponding -COOR ones **3e-6e** as expected



Scheme I - Schematic representation of the synthesis of the amino acid conjugates of *p*-*tert*-butyl-calix[4]arene and its –OMe analogue (a) BrCH₂COOEt, K₂CO₃, acetone, reflux 15 h (b) aq. NaOH, EtOH, reflux, 24 h (c) SOCl₂, benzene, reflux, 7 h (d) amino acid ester, HCl, NEt₃, THF, RT, 24 h (e) LiOH, THF/H₂O, except in case of the reaction going from **5e** to **5a** where Pd/C, H₂ were used. The suffix, 'e' is for ester and 'a' is for acid.

because the former are involved in extensive H-bonding to raise the melting temperature. In fact the formation of the amide bond present in the peptido-conjugates has been identified using FTIR spectra, wherein the amide I ($\nu_{C=O}$) and the amide II bands (δ_{NH}) appear in 1659–1688 cm⁻¹ and 1531–1539 cm⁻¹ respectively. The $\nu_{C=O}$ vibration observed in the 1740–1770 cm⁻¹ clearly differentiates the presence of ester moiety from that of the carboxylic moiety as the terminal groups of the arms, hence can be used as diagnostic to assess the end group of the arm. The ν_{OH} region showed a broad band comprising of both the phenolic –OH and the amide –NH vibrations.

¹H and ¹³C NMR studies

The proton and carbon resonances of amino acid portions of the conjugates were assigned based on ¹H-¹H COSY and ¹H-¹³C HMQC. The positions of amide proton signals were confirmed through cross coupling peaks of C^αH in COSY experiments. All the exchangeable proton resonances were cross checked from the spectra measured after D₂O addition. The chemical shifts observed in the present case were compared with those observed in case of the tetra-substituted amino acid ester derivatives¹³. The amide proton signals appeared downfield in the range 9.32 to 9.66 ppm (CDCl₃) for **3e-6e** and 8.72 to 9.14 ppm for **3a-6a** (DMSO-*d*₆), indicating the involvement of amide –NH in an intramolecular hydrogen bonding. The phenolic –OH protons were observed in the range, 7.73 to 7.97 ppm in case of **3e-6e** and 8.19 to 8.43 ppm in case of **3a-6a**.

The aromatic protons in **3e** appear as two singlets whereas those in **4e-6e** as two doublets of doublets. Similarly **3a** showed a sharp singlet at 7.17 ppm, **4e** and **6a** showed two doublets, **5a** showed one sharp doublet. This splitting is attributable to the presence of chiral C^α center present in the amino acid portion of the arms¹³. The axial and equatorial calixarene methylene bridged (CH₂) protons in **4e-6e** showed two pairs of doublets, unlike **3e**, due to the chiral nature of pendant amino acid groups. Similarly the diastereotopic nature of OCH_AH_B appeared as two doublets in case of **4e-6e**, but in case of **3e**, it appeared as a singlet. The methyl protons of the *tert*-butyl group in **3e-6e** appears as two singlets in the range 1.19–1.30 and 0.96–1.04 ppm and not much shifted in comparison to the precursor diacid. Similar splitting was observed even in the spectra of **3a-6a**. Thus the NMR spectral features were clearly indicative of the *cone*-conformation in all these conjugates.

The positions of the carbons arising from C^αH, C^βH (**4e-6e** and **4a-6a**), C^γH (**6e** and **6a**), OCH₂CO, Ar-CH₂-Ar were assigned by HMQC experiments. Results of ¹H-¹H COSY and ¹H-¹³C HMQC for **6e** and **6a** are shown in **Figure 1**. The peak corresponding to the ester carbonyl carbon (COOR, R = Me or Et or CH₂Ph) appeared at 169.5–173.3 ppm in **3e-6e**. An additional ester carbonyl peak appeared from side chain ester groups in case of **5e** and **6e**. The amide peak (–NH–CO) appeared at 168.7–169.2 ppm for **3e-6e**. Similarly in case of **3a-6a** the acid carbonyl (COOH) peak was found at 170.8–173.5 ppm and the

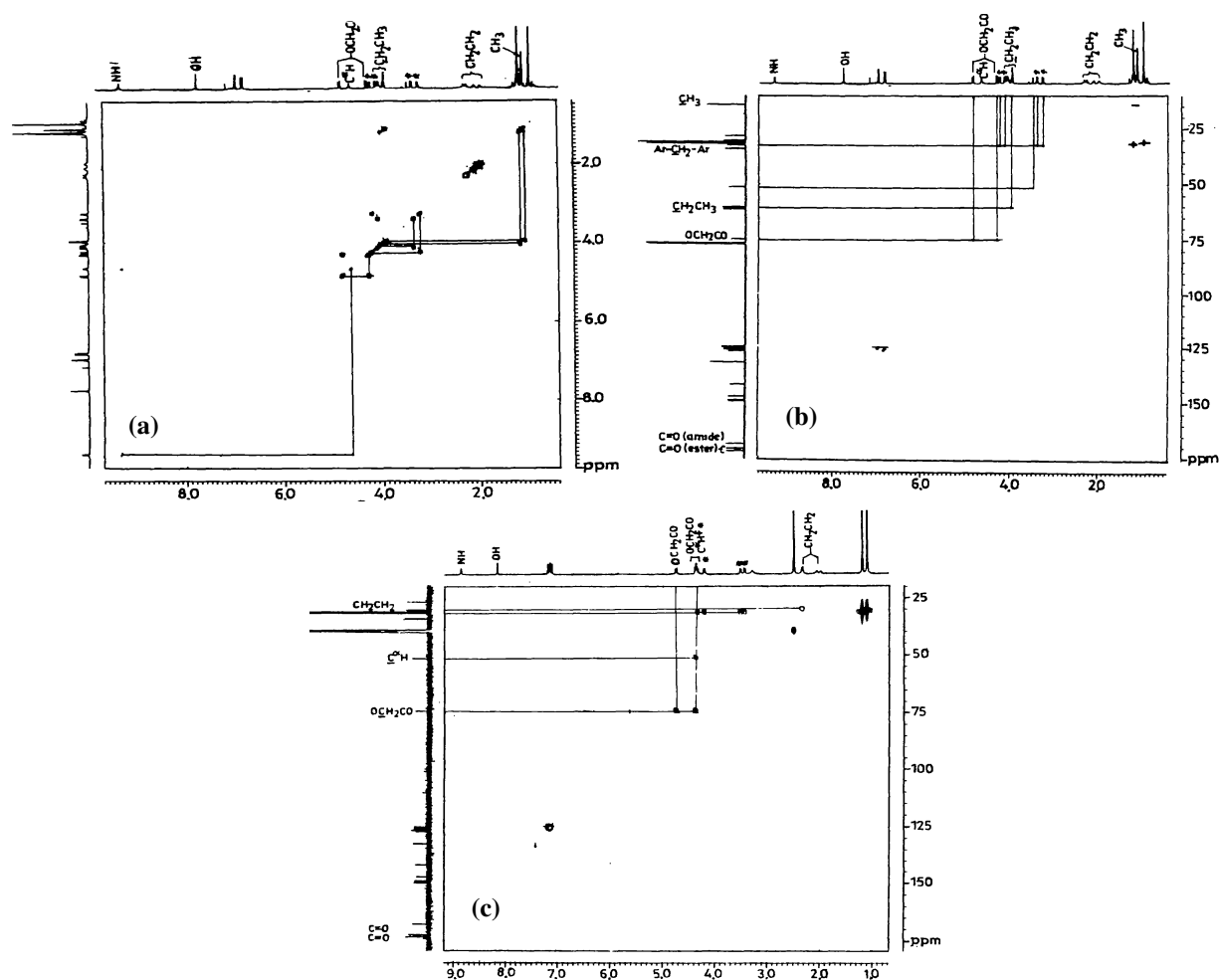


Figure 1: (a) ^1H - ^1H COSY and (b) ^1H - ^{13}C HMQC spectra for **6e** as recorded in $\text{DMSO-}d_6$ and (c) ^1H - ^{13}C HMQC for **6a** as recorded in $\text{DMSO-}d_6$. Selected assignments were marked on the corresponding one-dimensional spectrum and the cross peaks were connected.

amide carbonyl ($-\text{NH-CO}-$) peak at 167.7-168.4 ppm. The methylene group from OCH_2CO appeared at 74.8-74.9 ppm. Thus the structures of the conjugates shown in **Scheme I** were well supported by the NMR studies.

FAB MS studies: The mass spectra of all the conjugates showed molecular ion peaks corresponding to their molecular weights consistent with the formulae given in **Scheme I** based on the analytical data (**Table I**). Typical spectra for the glycine conjugates are shown in **Figure 2**. The spectra also exhibited some additional prominent peaks relevant to the fragments generated by the loss of arm(s) etc.

Single crystal XRD studies of **3e**

The molecular structure of **3e** has been established by single crystal XRD. Structural refinement and other data collection parameters for **3e** are

summarized in **Table II**. Molecular structure of **3e** and its intra-molecular hydrogen bonding formed by the pendants is shown in **Figure 3**. As evident from the crystal structure, the calix[4]arene derivative is in cone conformation where the amide-NH is involved in hydrogen bonding with the ether oxygen ($\text{N-H}\dots\text{O}_{\text{ether}}$) of the calix[4]arene pendants. Similarly phenolic-OH also forms hydrogen bond with ether oxygen ($\text{O-H}\dots\text{O}_{\text{ether}}$, 7-atom H-bond) and the amide-NH ($\text{N-H}\dots\text{O}_{\text{phenolic}}$, 10-atom H-bond) intra-molecularly. Amide oxygen of the pendent arm is involved in an intermolecular hydrogen bond with the aromatic hydrogen ($\text{C=O}\dots\text{H-C}_{\text{aromatic}}$) of a neighbour molecule as shown in **Figure 3b**. Lattice structure of **3e** is shown in **Figure 4a**. As evident from the figure that the structure resembles the cones arranged in antiparallel fashion and stacks one into the other as shown in line sketch of the lattice structure

(Figure 4b). Thus the *tert*-butyl group of calix[4]-arene moieties protrude into the hydrophobic core of the neighboring calix[4]arene. Since the bond lengths and bond angles of the conjugate were found to be normal, only those corresponding to the arms were given in Table III.

Conformational mobility induced by the replacement of lower rim phenolic–OH by –OCH₃, 7e-9e

As understood from the NMR spectral studies of these conjugates and the crystal structure of 3e, the *cone*-conformation is stabilized *via* the conformational turns formed by the pendant arms built through 11-atom intramolecular N-H...O interaction in addition to the intra-rim O-H...O interactions, all operating at the lower rim. This observation entrusted us with the synthesis of the corresponding conjugates where the two phenolic –OH groups were modified to –OCH₃ resulting in the compounds 7e-9e as shown in Scheme I. The products were thoroughly characterized. In these –OCH₃ derivatized conjugates, the *cone*-conformation is less favoured owing to the breakage of such H-bond interactions resulting in

conformational flexibility of the conjugates leading to the fluxional behaviour. While the RT ¹H NMR spectra were characteristic of dynamic phenomenon, the variable temperature study performed with 7e and 7a in the range -50°C to 110°C clearly indicated the fluxional behavior of these –OCH₃ derivatized conjugates. Selected portions of the spectra for 7a as a function of temperature are shown in Figure 5. The

Table II — Summary of crystallographic data and parameters for 3e

Parameters	3e
Empirical formula	C ₅₄ H ₇₀ N ₂ O ₁₀
Formula weight	907.12
Temperature	293(2) K
Wavelength/ Å	0.71073
Crystal system	Monoclinic
Space group	P2 ₁ /c
Cell constants	
<i>a</i> / Å	15.521(2)
<i>b</i> / Å	15.752(2)
<i>c</i> / Å	21.010(3)
β/deg	92.170(2)
Volume/ Å ³	5132.8(1)
Z	4
Calculated density/mgm ⁻³	1.174
Absorption coefficient/mm ⁻¹	0.080
F(000)	1952
Crystal size (mm ³)	0.3 x 0.2 x 0.1
Theta range (deg.)	1.31 to 25.00
Reflections collected	27133
Unique reflections	9041
Final R	0.0309
wR	0.1989

Table I — *m/z* Details for calix[4]arene derivatives

Compds	<i>m/z</i>	Compds	<i>m/z</i>
3e	906 [M] ⁺	3a	885 [M+Li] ⁺
4e	934 [M] ⁺	4a	913 [M+Li] ⁺
5e	1355 [M+H] ⁺	5a	995 [M+H] ⁺
6e	1135 [M+Na] ⁺	6a	1023 [M+H] ⁺
7e	935 [M+H] ⁺	7a	913 [M+Li] ⁺
8e	985 [M+Na] ⁺	8a	934 [M] ⁺
9e	1163 [M+H] ⁺	9a	1052[M+H] ⁺

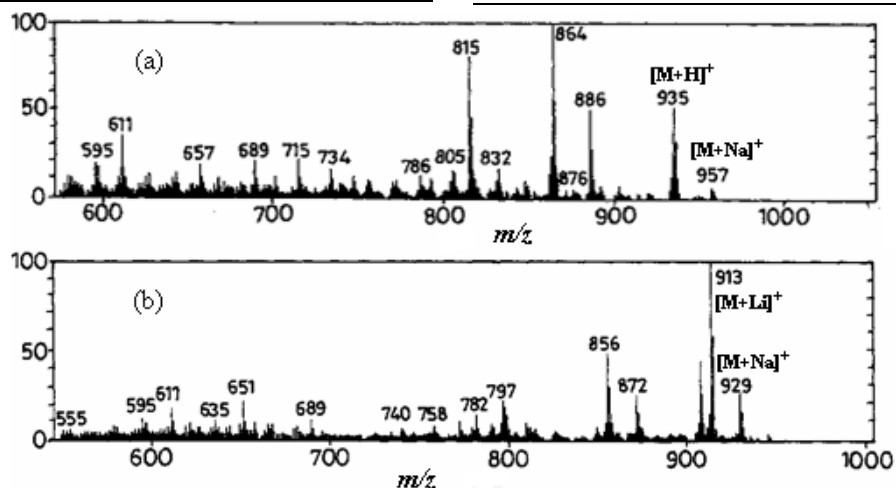


Figure 2: FAB mass spectra of (a) 7e and (b) 7a. M denotes the corresponding molecular ion.

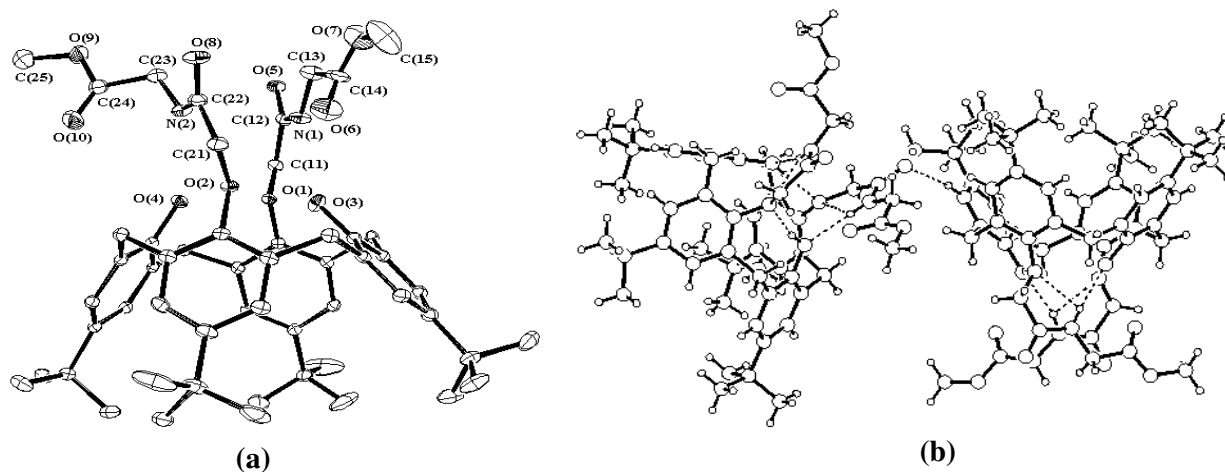


Figure 3 — Molecular Structure of **3e** (a) as an ORTEP plot, only pendant atoms are labeled and hydrogen atoms have been omitted for the sake of clarity and (b) intra and inter-molecular H-bonding in **3e**.

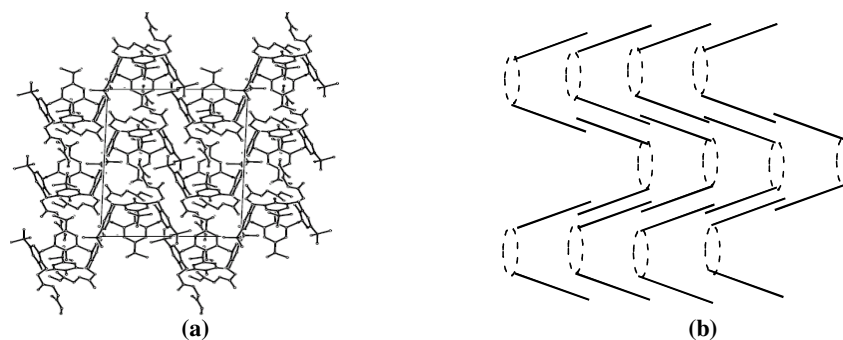


Figure 4 — (a) Packing of the **3e** in the lattice and (b) line diagram showing the stacking of calix[4]arene units in the lattice of **3e**.

data is consistent with a mixture of at least two conformers at room and low temperatures, but fits well with the presence of *cone*-conformation predominantly at 110°C. Fluxional behavior of one of the early precursors of the $-\text{OCH}_3$ conjugates, *viz.*, an ester precursor of **2a** in **Scheme I**, is reported in the literature¹⁴ and the fluxional behavior seems to continue even when the two arms were extended by amino acid *via* amide bonds, as observed in the present case. All this is possible when the intra-molecular interactions are disrupted to induce the pseudo rotation about the calix[4]arene at the lower rim.

Differential binding property of the carboxylic-acid and ester-end conjugates of calix[4]arene towards phosphate: Differential recognition of the peptido-conjugates reported in this paper towards phosphate monoester was demonstrated by performing binding studies using spectrophotometric

titrations. Addition of these conjugates, *viz.*, **3a**, **4a**, **6a** or **7a** to disodium salt of 4-nitrophenyl phosphate ($\text{Na}_2\text{-npp}$) at various phosphate to conjugate ratios in 1% $\text{H}_2\text{O-DMSO}$ resulted in dramatic change in the absorption spectrum wherein the absorbance of $\text{Na}_2\text{-npp}$ at 433 nm decreases and that at 312 nm increases with an isosbestic point being observed at 370 nm. Spectra observed during the titration are shown in **Figure 6a** in case of the conjugate **6a**. From the plot of absorbance of 433 nm band vs. concentration of the conjugate, the ratio of the resulting complex formed was determined. A typical plot for **6a** was shown in **Figure 6b**. The results suggest the formation of 1:1 complex in case of **3a-4a**, *i.e.*, with those amino acids having one $-\text{COOH}$ terminal group at each pendant and a 1:2 complex in case of **6a**, *viz.*, glu-conjugate possessing two $-\text{COOH}$ functions at the terminal of each pendant.

Table III — Selected bond lengths (Å) and bond angles (°) for the arm of **3e**

Bond	Length (Å)	Bond	Angle (°)
N(1)-C(12)	1.337(4)	C(12)-N(1)-C(13)	120.4(3)
N(1)-C(13)	1.452(4)	C(103)-O(1)-C(11)	115.5(2)
O(1)-C(103)	1.403(3)	C(302)-C(1)-C(102)	110.9(2)
O(1)-C(11)	1.431(3)	C(22)-N(2)-C(23)	123.0(3)
C(1)-C(302)	1.522(4)	C(203)-O(2)-C(21)	114.3(2)
C(1)-C(102)	1.523(4)	C(204)-C(2)-C(404)	109.8(2)
N(2)-C(22)	1.330(5)	C(304)-C(3)-C(202)	112.1(2)
N(2)-C(23)	1.441(4)	C(104)-C(4)-C(402)	111.0(2)

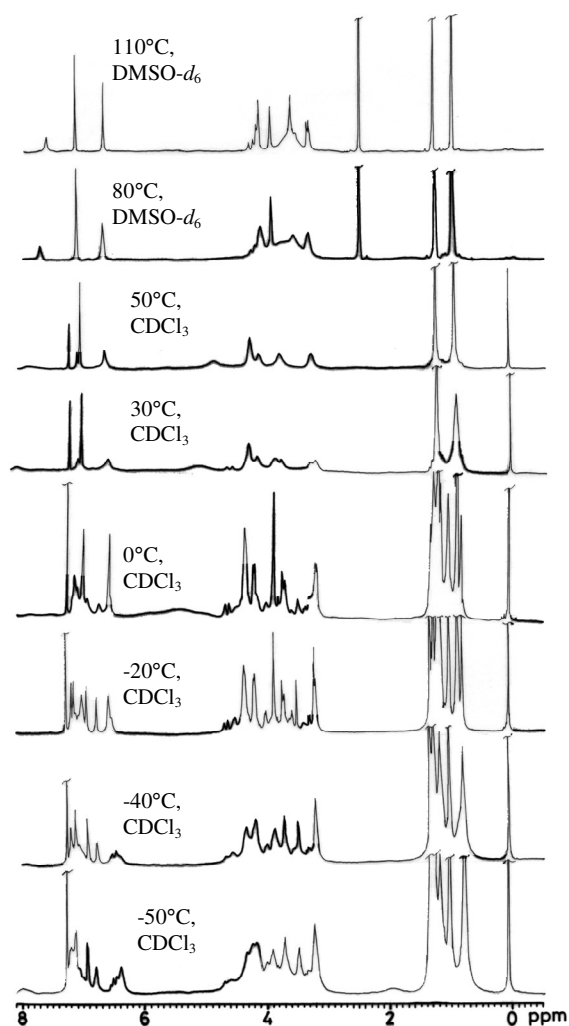


Figure 5 — ^1H NMR spectra of **7a**, indicating conformational mobility, as a function of temperature. Each spectral trace is labeled with the corresponding solvent and the temperature at which the spectrum is measured.

The binding constants were computed from the absorbance data¹⁵ and were found to be $(10 \pm 2) \times 10^5$, $(2.8 \pm 1) \times 10^5$, $(3.2 \pm 1) \times 10^5$ and $(3.3 \pm 1) \times 10^5 \text{ M}^{-1}$ for **3a**, **4a**, **6a** and **7a** respectively. Careful examination of the binding data, in comparison with that of the precursor calix-diacid, **1a₁** $\{(5.5 \pm 1.2) \times 10^5 \text{ M}^{-1}\}$, is

clearly suggestive of the interaction of the terminal –COOH group. The binding data is further influenced by the substitution at the C⁶ center of the amino acid moiety. The binding constants observed in the present case are certainly higher by at least two orders of magnitude when compared to the reported calix-

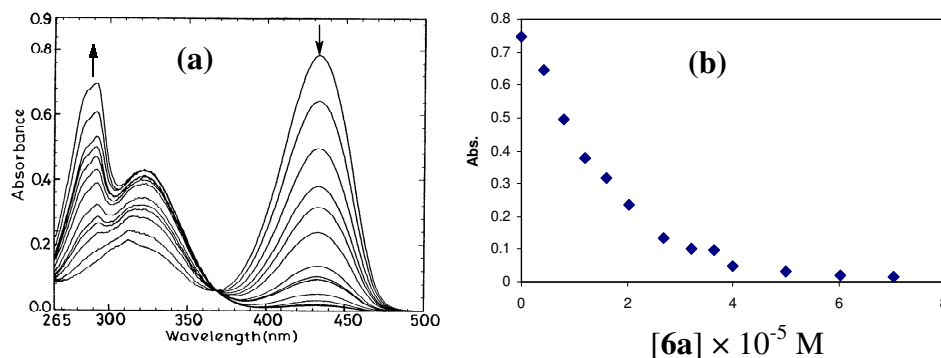


Figure 6 — (a) Absorption spectra of the titration between calix[4]arene-amino acid conjugate, **6a** and the phosphate, $\text{Na}_2\text{-npp}$ in 1% H_2O -DMSO. The upward and downward arrows indicate increase and decrease of the corresponding bands respectively. $[\text{Na}_2\text{-npp}] = 4 \times 10^{-5} \text{ M}$, $[\mathbf{6a}] = 0.42 \times 10^{-5}$ to $7.04 \times 10^{-5} \text{ M}$; (b) Plot of absorbance of 433nm band as a function of the concentration of the calix[4]arene-conjugate, **6a**.

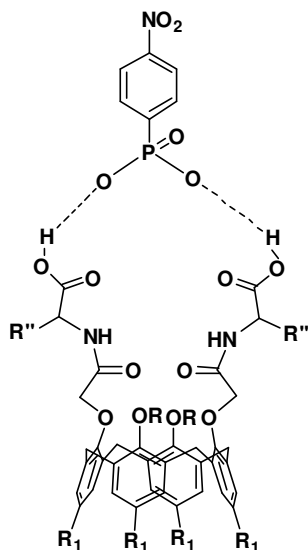


Figure 7 — Proposed model for phosphate binding with calix[4]arene-conjugate possessing end $-\text{COOH}$ group

cyclic peptide¹⁶. Based on these studies, the proposed model for phosphate binding with the $-\text{COOH}$ end conjugate was shown in **Figure 7**.

In case of the precursor ester-conjugates, viz., **3e**, **4e**, and **6e**, there do not seem to be any specific binding present, indicating that the $-\text{COOH}$ terminal is essential for recognition when the amide group is not accessible to the phosphate owing to its involvement in an intramolecular H-bond interaction as explained based on the structure in this paper. If this were to be true, in case of **7e** and **9e** where the phenolic $-\text{OH}$ groups were modified to $-\text{OCH}_3$ ($-\text{OCH}_3$ counter parts for **3e** and **6e**), this results in the breakage of the intramolecular H-bond of the amide-NH and hence is expected to show good binding

characteristics. Indeed the observed binding constants are, $(4.9 \pm 1.2) \times 10^5$ and $(5.0 \pm 1.2) \times 10^5 \text{ M}^{-1}$ respectively for **7e** and **9e** owing to the availability of amide-NH for interaction with the phosphate group. In contrast, the work reported in case of cyclic peptides¹⁵ possessing 6 to 14 peptide bonds exhibit low binding strength. Association between the phosphate and these conjugates is also evidenced from the ^1H NMR spectrum of the reaction between $\text{Na}_2\text{-npp}$ and **3a**, where the phenyl protons of the phosphate moiety exhibit a down-field shift of 1.1 ppm upon binding. Comparison of these results with appropriate control experiments involving *N*-acetylglutamic acid and *N*-*boc*-glycine further supports the interaction of terminal carboxylic groups with the phosphate moiety. Thus the $-\text{COOH}$ end conjugate recognizes the negatively charged phosphate group in preference over its $-\text{COOR}$ counterpart, as the former is driven through the hydrogen bond formation.

Conclusions

The idea of building 1,3-di-functional pendants on the calix[4]arene lower rim to provide a binding core has been well demonstrated through the formation of the peptido-conjugates of calix[4]arene as reported in this paper. Indeed these conjugates yielded a variable-type binding site with a built-in flexibility where the core can act as either N_2O_2 or N_2O_4 or even as N_2O_6 that may be suitable for binding transition or lanthanide ions. The *cone*-conformation has been observed owing to the intra-rim $\text{O-H}\dots\text{O}$ interactions operating at the lower rim. Breakage of such interactions indeed lead to the conformational

flexibility as demonstrated by us in case of the conjugates where the two phenolic-OH groups were replaced by the -OMe groups at the lower rim. The arms adapt a conformational turn by extending 11-atom hydrogen bond interaction between the amide NH and the rim-phenolic oxygen. Differential recognition characteristics of the calix-peptide conjugates towards phosphate anion were demonstrated. This was attributed to the hydrogen-bond association between the carboxylic terminal groups and/or the amide moiety depending upon the availability of these groups for interaction. The phosphate did not show any preferential interaction with the ester group **3e-3a**. Thus the present studies elicit an entry of this new series of calix[4]arene-peptido-conjugates into the field of molecular recognition.

Experimental Section

¹H and ¹³C NMR spectra were measured on a Varian Mercury NMR spectrometer working at 400 MHz. The mass spectra were recorded on Q-TOF micromass (YA-105) using electrospray ionization method. The absorption spectra were measured on JASCO V – 570. The elemental analyses were performed on ThermoQuest microanalysis. FT-IR spectra were measured on Perkin-Elmer spectrometer using KBr pellets. Single crystal X-ray diffraction data were measured on OXFORD XCALIBUR-S CCD machine. All the chemicals used were procured from Sigma Aldrich Chemical Co., U.S.A. All the solvents used were dried and distilled by usual procedures immediately before use. Distilled and de-ionized water was used in the studies.

p-*tert*-Butylcalix[4]arene conjugates, *viz.*, **3e-6e**, **7e-9e**, **3a-6a** and **7a-9a** shown in **Scheme I**, were synthesized using a reported procedure¹¹ with marginal modifications.

Characterization data for the conjugates

5,11,17,23-Tetra-*tert*-butyl-25,27-dihydroxy-26,28-bis(O-methyl-glycyl-carbonyl-methoxy)calix[4]arene (3e).—Yield: 70 %; m.p. 182°C (decomposes). FTIR (KBr): 3321 ($\nu_{\text{NH/OH}}$), 1754 ($\nu_{\text{C=O}}$, COOMe), 1685 ($\nu_{\text{C=O}}$, CONH) cm^{-1} ; ¹H NMR (CDCl₃): δ 1.03 (s, 18H, C(CH₃)₃), 1.27 (s, 18H, C(CH₃)₃), 3.43 (d, 4H, Ar-CH₂-Ar, J = 13.4 Hz), 3.72 (s, 6H, OCH₃), 4.14 (d, 4H, C ^{α} H, J = 4.95 Hz), 4.23 (d, 4H, Ar-CH₂-Ar, J = 13.3 Hz), 4.63 (s, 4H, O-CH₂-CO), 6.92 (s, 4H, Ar-H), 7.25 (s, 4H, Ar-H), 7.83 (s, 2H, OH), 9.27

(t, 2H, NH, J = 4.6, 4.7 Hz); ¹³C NMR (CDCl₃): δ 31.0, 31.6 (C(CH₃)₃), 32.1 (Ar-CH₂-Ar), 34.1, 33.9 (C(CH₃)₃), 41.2 (C ^{α} H), 52.3 (OCH₃), 74.8 (OCH₂CO), 125.5, 126.2, 127.1, 132.4, 142.9, 148.2, 149.2, 149.8 (aromatic carbons), 169.4 (C=O, CONH), 169.5 (C=O, COOCH₃); MS-EI: m/z 906 ([M]⁺, 100%). Anal. Calcd. for C₅₄H₇₀N₂O₁₀·H₂O (924): C, 70.13; H, 7.79; N, 3.03. Found: C, 70.66; H, 8.22; N, 2.87%.

5,11,17,23-Tetra-*tert*-butyl-25,27-dihydroxy-26,28-bis(O-methyl-R- α -alanyl-carbonyl-methoxy)calix[4]arene (4e).—Yield: 65 %; m.p. >240°C (decomposes). FTIR (KBr): 3337 ($\nu_{\text{NH/OH}}$), 1749 ($\nu_{\text{C=O}}$, COOMe), 1680 ($\nu_{\text{C=O}}$, CONH) cm^{-1} ; ¹H NMR (CDCl₃): δ 0.97, 1.28 (s, 18H each, C(CH₃)₃), 1.47 (d, 6H, CH₃, J = 7.21 Hz), 3.40 (d, 2H, Ar-CH₂-Ar, J = 13.3 Hz), 3.46 (d, 2H, Ar-CH₂-Ar, J = 13.5 Hz), 3.69 (s, 6H, OCH₃), 4.18 (d, 2H, Ar-CH₂-Ar, J = 13.2 Hz), 4.31 (d, 2H, Ar-CH₂-Ar, J = 13.5 Hz), 4.53 (d, 2H, CH₂-O, J = 15.2 Hz), 4.74-4.69 (m, 2H of C ^{α} H and 2H of O-CH₂-CO), 6.93 (d, 4H, Ar-H), 7.08 (d, 4H, Ar-H), 7.85 (s, 2H, OH), 9.42 (d, 2H, NH, J = 7.43 Hz) ppm; ¹³C NMR (CDCl₃): δ 17.9 (CH₃ of ala), 30.9, 31.6 (C(CH₃)₃), 32.1, 32.3 (Ar-CH₂-Ar), 33.9, 34.1 (*tert*-C), 48.0 (C ^{α} H), 52.3 (OCH₃), 74.8 (O-CH₂-CO), 125.4, 125.5, 126.2, 127.1, 127.2, 132.4, 132.5, 142.8, 148.2, 149.60, 149.64 (aromatic carbons), 168.7 (C=O, CONH), 172.6 (C=O, COOMe); MS-EI: m/z 934 ([M]⁺, 95%). Anal. Calcd. for C₅₆H₇₄N₂O₁₀ (934): C, 71.95; H, 7.92; N, 3.00. Found: C, 71.34; H, 7.71; N, 3.10%.

5,11,17,23-Tetra-*tert*-butyl-25,27-dihydroxy-26,28-bis(O-benzyl-R- α -aspartyl-carbonyl-methoxy)calix[4]arene (5e).—Yield 54%. FTIR (KBr): 3323, 1749 ($\nu_{\text{C=O}}$, COOPh); 1680 ($\nu_{\text{C=O}}$, CONH) cm^{-1} ; ¹H NMR (CDCl₃): δ 1.04, 1.24 (s, 36H each, C(CH₃)₃), 2.97 (t, 2H, C ^{β} H-asp, J = 5.1 Hz), 3.24 (d, 2H, Ar-CH₂-Ar, J = 13.0 Hz), 3.42 (d, 2H, Ar-CH₂-Ar, J = 13.7 Hz), 4.14 (d, 2H, Ar-CH₂-Ar, J = 13.7 Hz), 4.29 (d, 2H, Ar-CH₂-Ar), 4.37 (d, 2H, OCH₂CO, 12.4 Hz), 4.77 (d, 2H, OCH₂CO, J = 12.4 Hz), 5.03 (m, H, C ^{α} H-asp + OCH₂Ph), 7.92 (s, 2H, OH), 9.63 (d, 2H, NH, J = 7.1 Hz); ¹³C NMR (CDCl₃): δ 31.0, 31.6 (C(CH₃)₃), 32.2, 32.4 (Ar-CH₂-Ar), 33.8, 34.1 (*tert*-C), 37.1, 49.4 (C ^{β} H), 66.4 (OCH₂CO), 67.3 (C ^{α} H), 75.0, (OCH₂Ph), 125.1, 125.4, 125.7, 126.5, 126.8, 127.7, 128.09, 128.1, 128.3, 128.4, 132.4, 132.7, 135.5, 135.7, 142.5, 147.9, 149.8, 150.0 (aromatic carbons), 169.2 (C=O, CONH), 169.5 (C=O,

COOPh), 170.0 (C=O, COOPh); FABMS: m/z 1355 ($[M+H]^+$, 90%); 1377 ($[M+Na]^+$, 50%). Anal. Calcd. for $C_{84}H_{94}N_2O_{14}$ (1354): C, 74.45; H, 6.94; N, 2.07. Found: C, 74.14; H, 7.34; N, 1.73%.

5,11,17,23-Tetra-tert-butyl-25,27-dihydroxy-26,28-bis(O-ethyl-R- α -glutyl-carbonylmethoxy)calix[4]arene (6e). —Yield 84%; m.p. 168-170°C. FT-IR (KBr): 3362, 3312(ν_{OH}); 1741 ($\nu_{C=O}$, COOEt) 1685 ($\nu_{C=O}$, CONH) cm^{-1} ; 1H NMR ($CDCl_3$): δ 0.96 (s, 18H, $C(CH_3)_3$), 1.10 (t, 6H, CH_2-CH_3 , $J = 7.1$ Hz), 1.18 (t, 6H, CH_2-CH_3), 1.19 (s, 18H, $C(CH_3)_3$), 1.97 (m, 2H, CH_2-CH_3), 2.10 (m, 2H, CH_2-CH_2), 2.29 (m, 4H, CH_2-CH_2), 3.26 (d, 2H, Ar- CH_2 -Ar, $J = 13.0$ Hz), 3.40 (d, 2H, Ar- CH_2 -Ar, $J = 13.6$ Hz), 3.97 (q, 4H, CH_2-CH_2 , $J = 7.1$ Hz), 4.13 (d, 2H, Ar- CH_2 -Ar, $J = 13.6$ Hz), 4.24 (d, 2H, Ar- CH_2 -Ar, $J = 12.9$ Hz), 4.31 (d, 2H, O- CH_2 -CO, $J = 15.2$ Hz), 4.65 (q, 2H, $C^\alpha H$ -glu, $J = 7.0$ Hz), 4.85 (d, 2H, O- CH_2 -CO, $J = 15.2$ Hz), 6.83 (d, 4H, Ar-H), 6.99 (d, 4H, Ar-H), $J = 7.15$ Hz), 7.78 (s, 2H, -OH), 9.37 (d, 2H, -NH-); ^{13}C NMR ($CDCl_3$): δ 14.11, 14.13 (CH_2-CH_3), 28.1 (*tert*-C), 30.3 (*tert*-C), 30.9, 31.6 ($C(CH_3)_3$), 32.2, 32.3 (Ar- CH_2 -Ar), 33.8, 34.0 (*tert*-C), 60.4 (CH_2-CH_3), 61.3 (*tert*-C), 74.9 (O- CH_2 -CO), 125.2, 125.6, 125.7, 126.5, 126.7, 127.3, 132.5, 142.5, 148.0, 149.6, 150.0 (aromatic carbons), 169.0 (C=O, CONH), 171.2 (C=O, COOEt), 173.3 (C=O, COOEt); FABMS: m/z 1135 ($[M+H]^+$, 100%); 1157 ($[M+Na]^+$, 30%). Anal. Calcd. for $C_{66}H_{90}N_2O_{14}$ (1134): C, 69.84; H, 7.94; N, 2.47. Found: C, 69.25; H, 8.46; N, 2.38%.

5,11,17,23-Tetra-tert-butyl-25,27-dihydroxy-26,28-bis(glycyl carbonylmethoxy)calix[4]arene (3a). —Yield 89 %; m.p. 210°C (decomposes). FTIR (KBr): 1743 ($\nu_{C=O}$, COOH); 1668 ($\nu_{C=O}$, CONH) cm^{-1} ; 1H NMR ($DMSO-d_6$): δ 1.13 (s, 18H, $C(CH_3)_3$), 1.20 (s, 18H, $C(CH_3)_3$), 3.47 (d, 4H, Ar- CH_2 -Ar, $J = 13.2$ Hz), 4.03 (m, 4H, $C^\alpha H_2$), 4.23 (d, 4H, Ar- CH_2 -Ar, $J = 12.8$ Hz), 4.53 (s, 4H, OCH_2CO), 7.17 (s, 8H, Ar-H), 8.41 (s, 2H, OH), 8.89 (t, 2H, HN) ppm; ^{13}C NMR ($DMSO-d_6$): δ 30.8, 31.3 ($C(CH_3)_3$), 33.6, 34.0 ($C(CH_3)_3$), 40.6 ($C^\alpha H_2$), 67.0 (*tert* C), 74.0 (OCH_2CO), 125.5, 125.9, 126.9, 132.8, 141.6, 147.5, 149.6, 149.9 (aromatic carbons), 168.4 (C=O, CONH), 170.8 (C=O, COOH); FABMS: m/z 885 ($[M+Li]^+$, 90%). Anal. Calcd. for $C_{52}H_{66}N_2O_{10} \cdot 3H_2O$ (932): C, 66.93; H, 7.78; N, 3.00. Found: C, 66.71; H, 7.72; N, 2.86%.

5,11,17,23-Tetra-tert-butyl-25,27-dihydroxy-26,28-bis(R- α -alanyl-carbonylmethoxy)-calix[4]arene (4a). —Yield 93%; m.p. 196-198 °C. FTIR (KBr):

3434, 3343, 1741 ($\nu_{C=O}$, COOH); 1660 ($\nu_{C=O}$, CONH) cm^{-1} ; 1H NMR ($DMSO-d_6$): δ 1.12 (s, 18H, $C(CH_3)_3$), 1.20 (s, 18H, $C(CH_3)_3$), 1.40 (d, 6H, CH_3 -ala, $J = 7.27$ Hz), 3.45 (d, 2H, Ar- CH_2 -Ar, $J = 12.9$ Hz), 3.54 (d, 2H, Ar- CH_2 -Ar, $J = 13.1$ Hz), 4.15 (d, 2H, Ar- CH_2 -Ar, $J = 13.1$ Hz), 4.31 (d, 2H, OCH_2CO , $J = 15.1$ Hz), 4.41-4.36 (m, 2H each, Ar- CH_2 -Ar + $C^\alpha H$), 4.77 (d, 2H, OCH_2CO , $J = 15.1$ Hz), 7.22-7.17 (m, 8H, Ar-H), 8.30 (s, 2H, OH), 9.09 (d, 2H, HN, $J = 7.6$ Hz); ^{13}C NMR ($DMSO-d_6$): δ 16.9($C^\beta H_3$), 30.7, 31.3 ($C(CH_3)_3$), 30.8 (Ar- CH_2 -Ar), 31.5 (Ar- CH_2 -Ar), 33.6, 34.0 ($C(CH_3)_3$), 47.8 ($C^\alpha H$), 74.4 (OCH_2CO), 125.4, 125.6, 125.8, 126.4, 126.7, 127.4, 132.6, 132.9, 142.0, 147.7, 149.3, 150.0 (aromatic carbons), 167.7 (C=O CONH), 173.7 (C=O COOH); FABMS: m/z 913 ($[M+Li]^+$, 95%). Anal. Calcd. for $C_{54}H_{70}N_2O_{10} \cdot 4H_2O$ (978): C, 66.23; H, 8.03; N, 2.86. Found: C, 66.40; H, 7.73; N, 2.67%.

5,11,17,23-Tetra-tert-butyl-25,27-dihydroxy-26,28-bis(R- α -aspartyl-carbonylmethoxy)calix[4]arene (5a). —Yield 85%; m.p. 166-168°C. FTIR (KBr): 3433 (br, $\nu_{NH/OH}$); 1738 ($\nu_{C=O}$, COOH); 1655 ($\nu_{C=O}$, CONH) cm^{-1} ; 1H NMR ($DMSO-d_6$): δ 1.17 (s, 18H, $C(CH_3)_3$), 1.20 (s, 18H, $C(CH_3)_3$), 2.81-2.78 (m, 4H, $C^\beta H_2$ -Ph), 3.43 (d, 4H, Ar- CH_2 -Ar), 4.26 (t, 4H, Ar- CH_2 -Ar), 4.61 (m, 4H, OCH_2CO), 4.76 (q, 2H, $C^\alpha H$, $J = 7.6$ Hz), 7.14 (d, 8H, Ar-H, $J = 6.22$ Hz), 8.20 (s, 2H, OH), 8.88 (d, 2H, NH, $J = 7.85$ Hz); ^{13}C NMR ($DMSO-d_6$): δ 30.8, 31.3 ($C(CH_3)_3$), 33.5, 33.9 ($C(CH_3)_3$), 35.9 ($C^\beta H_2$ -Ph), 48.6 ($C^\alpha H$), 74.1 (OCH_2CO), 125.4, 125.8, 127.0, 141.5, 147.2, 149.6, 150.5 (aromatic carbons), 168.0 (C=O CONH), 171.6, 171.9 (C=O, COOH); FABMS: m/z 995 ($[M+H]^+$, 20%). Anal. Calcd. for $C_{56}H_{70}N_2O_{14} \cdot 3H_2O$ (1048): C, 64.12; H, 7.25; N, 2.67. Found: C, 63.78; H, 7.02; N, 3.01%.

5,11,17,23-Tetra-tert-butyl-25,27-dihydroxy-26,28-bis(R- α -glutyl-carbonylmethoxy)-calix[4]arene, (6a). —Yield 87 %; m.p. 172°C. FTIR (KBr): 3436, 3310, 1733 ($\nu_{C=O}$, COOH); 1660 ($\nu_{C=O}$, CONH) cm^{-1} ; 1H NMR ($DMSO-d_6$): δ 1.11 (s, 18H, $C(CH_3)_3$), 1.20 (s, 18H, $C(CH_3)_3$), 1.99-2.08 (m, 4H, $C^\beta H$), 2.32-2.36 (m, 4H, $C^\gamma H$), 3.44 (d, 2H, Ar- CH_2 -Ar, $J = 12.9$ Hz), 3.51 (d, 2H, Ar- CH_2 -Ar, $J = 13.2$ Hz), 4.21 (d, 2H, Ar- CH_2 -Ar, $J = 13.1$ Hz), 4.40-4.33 (m, 6H, 2H each of OCH_2CO , $C^\alpha H$, Ar- CH_2 -Ar), 4.75 (d, 2H, OCH_2CO , $J = 14.9$ Hz), 7.20-7.12 (m, 8H, Ar-H), 8.17 (s, 2H, OH), 8.87 (d, 2H, NH, $J = 7.2$ Hz); ^{13}C NMR ($DMSO-d_6$): δ 26.3, 29.9 (CH_2-CH_2), 30.7, 31.3

(C(CH₃)₃), 33.6, 33.9 (C-*tert*), 51.4 (C^αH), 74.2 (OCH₂CO), 125.4, 125.7, 126.2, 126.7, 127.2, 132.6, 132.7, 147.5, 149.4, 141.9, 150.2 (aromatic carbons), 168.0 (C=O, CONH), 172.6 (C=O, COOH), 173.5 (C=O, COOH); FABMS: *m/z* 1023 ([M+H]⁺, 50%), 1045 ([M+Na]⁺, 20%). Anal. Calcd. for C₅₈H₇₄N₂O₁₄.H₂O (1040): C, 66.92; H, 7.31; N, 2.69. Found: C, 66.49; H, 7.18; N, 2.08%.

5,11,17,23-Tetra-*tert*-butyl-25,27-dimethoxy-26,28-bis(O-methyl glycylicarbonylmethoxy)calix[4]-arene (7e). —Yield: 51%; m.p. 220°C (decomposes). FT-IR (KBr): 3412 (ν_{NH/OH}), 1754 (ν_{C=O}, COOMe), 1687 (ν_{C=O}, CONH) cm⁻¹; ¹H NMR (CDCl₃): δ 9.27 (t, *J* = 4.6, 4.7 Hz, 2H, NH), 7.25 (s, 4H, Ar-H), 6.92 (s, 4H, Ar-H), 4.63 (s, 4H, O-CH₂-CO), 4.23 (d, *J* = 13.3 Hz, 4H, Ar-CH₂-Ar), 4.14 (d, *J* = 4.95 Hz, 4H, C^αH), 3.85 (s, 6H, Ph-OCH₃), 3.72 (s, 6H, OCH₃), 3.43 (d, *J* = 13.4 Hz, 4H, Ar-CH₂-Ar), 1.27 (s, 18H, C(CH₃)₃), 1.03 (s, 18H, C(CH₃)₃); ¹³C NMR (CDCl₃): δ 31.0, 31.6 (C(CH₃)₃), 32.1 (Ar-CH₂-Ar), 33.9, 34.1 (C(CH₃)₃), 41.2 (C^αH), 52.3 (OCH₃), 74.8 (OCH₂CO), 125.5, 126.2, 127.1, 132.4, 142.9, 148.2, 149.2, 149.8 (Ar-C), 169.4 (CONH), 169.5 (COOMe); ESI MS: *m/z* 935 ([M+H]⁺, 60%), 957 ([M+Na]⁺, 10%). Anal. Calcd. for C₅₆H₇₄N₂O₁₀ (934): C, 71.95; H, 7.92; N, 3.00. Found: C, 71.52; H, 8.27; N, 2.73%.

5, 11, 17, 23 -Tetra-*tert*-butyl-25,27-methoxy-26,28-bis(O-methyl-R-α-alanyl-carbonylmethoxy)calix[4]arene (8e). —Yield: 45%; m.p. >250°C. FTIR (KBr): 3421 (ν_{NH/OH}), 1749 (ν_{C=O}, COOMe), 1688 (ν_{C=O}, CONH) cm⁻¹; ESI MS: *m/z* 985 ([M+Na]⁺, 100%). Anal. Calcd. for C₅₈H₇₈N₂O₁₀.H₂O (980): C, 71.02; H, 8.16; N, 2.86. Found: C, 70.69; H, 7.92; N, 3.05%.

5,11,17,23-Tetra-*tert*-butyl-25,27-dimethoxy-26,28-bis(O-ethyl-R-α-glutyl-carbonylmethoxy)calix[4]arene (9e). —Yield: 54%; m.p. 150°C. FTIR (KBr): 3414(ν_{OH}), 1744 (ν_{C=O}, COOEt), 1691 (ν_{C=O}, CONH) cm⁻¹. FABMS: *m/z* 1163 ([M+H]⁺, 30%). Anal. Calcd. for C₆₂H₆₈N₂O₁₄ (1162): C, 70.22; H, 8.09; N, 2.41. Found: C, 69.77; H, 8.53; N, 2.99%.

5,11,17,23-Tetra-*tert*-butyl-25,27-dimethoxy-26,28-bis(glycyl carbonylmethoxy)calix-[4]arene (7a). —Yield: 79%; m.p. 170-172°C. FT-IR (KBr): 3421, 3332 (ν_{OH/NH}), 1743 (ν_{C=O}, COOH), 1660 (ν_{C=O}, CONH) cm⁻¹; FABMS: *m/z* 913 ([M+Li]⁺, 100%), 929 ([M+Na]⁺, 30%). Anal. Calcd. for C₅₄H₇₀N₂O₁₀.H₂O (924): C, 71.52; H, 7.73; N, 3.09. Found: C, 70.98; H, 8.14; N, 2.75%.

5,11,17,23-Tetra-*tert*-butyl-25,27-dimethoxy-26,28-bis(R-α-alanyl-carbonylmethoxy)-calix[4]arene (8a). —Yield: 29%; m.p. >250°C. FT-IR (KBr): 3421, 3353 (ν_{OH/NH}), 1739 (ν_{C=O}, COOH), 1601 (ν_{C=O}, CONH) cm⁻¹; FABMS: *m/z* 934 ([M]⁺, 70%). Anal. Calcd. for C₅₆H₇₄N₂O₁₀ (924): C, 71.95; H, 7.92; N, 3.00. Found: C, 71.61; H, 7.48; N, 2.64%.

5,11,17,23-Tetra-*tert*-butyl-25,27-dihydroxy-26,28-bis(R-α-glutyl-carbonylmethoxy)calix[4]arene (9a). —Yield: 85%; m.p. 200°C (decomposes). FTIR (KBr): 3404, 1739 (ν_{C=O}, COOH), 1678 (ν_{C=O}, CONH) cm⁻¹; ¹H NMR (DMSO-*d*₆): δ 1.11 (s, 18H, C(CH₃)₃), 1.20 (s, 18H, C(CH₃)₃), 1.99-2.08 (m, 4H, C^βH), 2.32-2.36 (m, 4H, C^γH), 3.44 (d, 2H, Ar-CH₂-Ar, *J* = 12.9 Hz), 3.51 (d, 2H, Ar-CH₂-Ar, *J* = 13.2 Hz), 3.85 (s, 6H, Ph-OCH₃), 4.21 (d, 2H, Ar-CH₂-Ar, *J* = 13.1 Hz), 4.40-4.33 (m, 6H, 2H each of OCH₂CO, C^αH, Ar-CH₂-Ar), 4.75 (d, 2H, OCH₂CO, *J* = 14.9 Hz), 7.20-7.12 (m, 8H, Ar-H), 8.17 (s, 2H, OH), 8.87 (d, 2H, NH, *J* = 7.2 Hz); ¹³C NMR (DMSO-*d*₆): δ 26.3, 29.9 (CH₂-CH₂), 30.7, 31.3 (C(CH₃)₃), 33.6, 33.9 (C-*tert*), 51.4 (C^αH), 74.2 (OCH₂CO), 125.4, 125.7, 126.2, 126.7, 127.2, 132.6, 132.7, 147.5, 149.4, 141.9, 150.2 (aromatic carbons), 168.0 (C=O, CONH), 172.6 (C=O, COOH), 173.5 (C=O, COOH); FABMS: *m/z* 1052([M+H]⁺, 85%). Anal. Calcd. for C₆₀H₇₈N₂O₁₄.H₂O (1068): C, 67.42; H, 7.49; N, 2.62. Found: C, 67.19; H, 6.98; N, 2.21%.

Phosphate binding studies

Binding of 4-nitrophenyl phosphate (Na₂-npp) with the conjugates of calix[4]arene at 25°C has been studied by following the absorbance of the 433 nm band. In order to increase the solubility of Na₂-npp, these experiments were carried out in 1% H₂O-DMSO at a fixed concentration of Na₂-npp. In a typical experiment, Na₂-npp (4.0 × 10⁻⁵ M) and the calixarene-amino acid conjugate, (0.42 × 10⁻⁵ - 24.02 × 10⁻⁵ M) in 1% H₂O-DMSO were mixed and the UV/Vis absorption spectra were measured at each addition of the conjugate (each ratio was made freshly) until no substantial decrease was observed in the absorbance of the 433 nm band. Simultaneously, the band at 312 nm increased with an isosbestic point being observed at 370 nm. The ratio of the resulting complex formed was determined from the plot of the measured absorbance at 433 nm versus concentration of calix-amino acid conjugate. The binding constants were then computed from the absorbance data using Benesi-Hildebrand method¹⁷.

Acknowledgements

One of the author CPR acknowledges the financial support from DST, CSIR and BRNS-DAE. MD, AA and AA acknowledge CSIR for their senior research fellowships. We thank SAIF, IIT Bombay for some spectral measurements.

References

- 1 Gutsche C D, *Calixarenes Revisited, Monographs in Supramolecular Chemistry*, edited by J F Stoddart (Royal Society of Chemistry, Cambridge), **1998**.
- 2 Asfari Z, Bohmer V, Harrowfield J M & Vicens J, *Calixarenes* (Kluwer Academic Publishers, Dordrecht), **2001**.
- 3 Bohmer V, *Angew Chem Int Ed Engl*, **34**, **1995**, 713.
- 4 Shinkai S, *Tetrahedron*, **49**, **1993**, 8933.
- 5 Molenveld P, Kapsabelis S, Engberson J F J & Reinhoudt D N, *J Am Chem Soc*, **119**, **1997**, 2948.
- 6 Molenveld P, Engberson J F J, Kooijnean H, Spek A L & Reinhoudt D N, *J Am Chem Soc*, **129**, **1998**, 6726.
- 7 Barrett G, Corry D, Creaven B S, Johnston B, McKerverly M A & Rooney A, *J Chem Soc, Chem Commun*, **1995**, 363.
- 8 Schneider H -J & Schneider U, *J Incl Phenom Mol Recogn Chem*, **19**, **1994**, 67.
- 9 Shinkai S, Koreishi H, Ueda K, Arimura T & Manabe O, *J Am Chem Soc*, **109**, **1987**, 6371.
- 10 Collins E M, McKerverly M A, Madigan E, Moran M B, Owens M, Ferguson G & Harris S J, *J Chem Soc, Perkin Trans, 1*, **1991**, 3137.
- 11 Rao P V, Rao C P, Kolehmainen E, Wegelius E K & Rissanen K, *Chem Lett*, **2001**, 1176.
- 12 Sabbatini N, Casnati A, Fischer C, Girardini R, Guardigli M, Manet I, Sarti G & Ungaro R, *Inorg Chim Acta*, **252**, **1996**, 19.
- 13 Sansone F, Barbosa S, Casnati A, Fabbi M, Pochini A, Ugozzoli F & Ungaro R, *Eur J Org Chem*, **1998**, 897.
- 14 Duggan P J, Sheahan S L & Szydzik M L, *Tetrahedron Lett*, **41**, **2000**, 3165.
- 15 Ishida H, Suga M, Donowaki K & Ohkubo K, *J Org Chem*, **60**, **1995**, 5374.
- 16 Hu X, Chan A S C, Han X, He J & Cheng J -P, *Tetrahedron Lett*, **40**, **1999**, 7115.
- 17 Benesi H A & Hildebrand J H, *J Am Chem Soc*, **71**, **1949**, 2703.